

Deep-level symmetry studies using ballistic-phonon transmission in undoped semi-insulating GaAs

J. C. Culbertson, U. Strom, and S. A. Wolf
Naval Research Laboratory, Washington D.C. 20375
 (Received 2 March 1987)

An anisotropic change in ballistic-phonon transmission induced by irradiation with 1.06- μm -wavelength photons has been measured in undoped semi-insulating GaAs. The anisotropy of the phonon transmission is consistent with scattering from a defect having trigonal symmetry. The metastability, as well as the thermal-annealing and optical-excitation properties of the observed change in phonon transmission, are consistent with those which have been associated with the dominant deep electronic level (*EL2*) in undoped semi-insulating GaAs.

Undoped semi-insulating GaAs is a material of considerable scientific and technological interest. Much of the scientific interest has been focused on understanding the nature of the intrinsic defect states in this material. It is now well established that the As_{Ga} antisite defect (As on a Ga site) is an important intrinsic defect. This defect appears to be closely associated with the ubiquitous deep donor *EL2*, which is thought to render GaAs semi-insulating. There is a broad consensus that As_{Ga} constitutes part of a more extended *EL2* defect, or a family of *EL2* defects. The determination of the structural details of these extended defects in GaAs has been difficult by means of traditional probes of the local environment, such as electron spin resonance (ESR).

Information about the local symmetry of a defect can be obtained from ballistic-phonon transport measurements. Such a technique was used successfully to determine the symmetry of Cr defects in GaAs.¹ These results were subsequently confirmed by an acoustic-phonon relaxation experiment.² The interpretation of experimental phonon scattering data relies on the prediction of group theory that a defect can scatter phonons anisotropically only if the defect has a symmetry that is lower than that of the lattice position it occupies.³ The nature of the anisotropic scattering can be calculated for defects of various symmetries.

This Rapid Communication describes the first measurements of defect-related anisotropic phonon transport in undoped liquid-encapsulated-Czochralski- (LEC) grown semi-insulating GaAs. The GaAs crystal (obtained from Microwave Associates) was grown in a BN crucible with a B_2O_3 encapsulant and an overpressure of As — conditions under which the presence of the *EL2* defect is expected. Optical-absorption measurements are consistent with a concentration of *EL2* of $(1-2) \times 10^{16} \text{ cm}^{-3}$. ESR measurements at 15 K have been performed to determine the concentration of As_{Ga} in the $1+$ charge state $[\text{As}_{\text{Ga}}]^+ \approx (1-2) \times 10^{16} \text{ cm}^{-3}$. This provides a lower bound on the concentration of As_{Ga} . If *EL2* contains an As_{Ga} , as is presently believed, then the total concentration of As_{Ga} is an upper bound on the concentration of *EL2*.

Our ballistic-phonon studies were performed on a 0.5-mm-thick piece of grown GaAs. A square NbN granular superconducting bolometer,^{4,5} $\frac{1}{2}$ mm on a side, was de-

posited on one (100) surface of this crystal and a thin light-absorbing film was evaporated onto the opposing surface. The film consists of 30 Å of Cr followed by 500 Å of Al and 200 Å of Ge. Heat pulses were created by focusing light pulses onto the film (5800-Å wavelength, 6-ns duration, and 2–50 nJ/pulse). This film is opaque to the 5800-Å light. To observe the [100] phonon transport the laser beam was focused (spot size $\sim 150 \mu\text{m}$) on the film directly opposite the bolometer. The GaAs crystal was sufficiently transparent to phonons to allow a substantial fraction of the heat pulse to traverse the crystal without scattering (ballistic transport). To measure transport along the [110] and [111] directions the laser beam was moved along the film. All measurements were made at 2 K.

Figure 1(a) shows the bolometer response for phonon propagation along the [100] direction. The longitudinal-acoustic (LA) and transverse-acoustic (TA) phonons are so labeled. The 6-ns-long, heat-generating optical pulse occurs at zero time. The arrival times (onsets) of the ballistic $\text{TA}_{[100]}$ and $\text{LA}_{[100]}$ phonons agree well with those predicted by dividing our crystal's thickness by the accepted $\text{TA}_{[100]}$ and $\text{LA}_{[100]}$ phonon sound velocities.

The solid line in Fig. 1(a) is the heat pulse observed before irradiation with 1.06- μm light. The dashed curve is the heat pulse measured after a 5-min irradiation with 5 mW cm^{-2} of 1.06- μm -wavelength light at 2 K. *This change in phonon signal is observed only when the sample is irradiated with photons whose energies lies within the range from 1.0 to 1.2 eV.*⁶ This corresponds closely to the intracenter absorption band of the deep level *EL2*. This change in phonon transmission is metastable at low temperatures. Raising the temperature above 130 K restores the initially smaller phonon pulse amplitude. We also verified that the bolometer resistance had not changed after exposure to 1.06- μm light. Thus we conclude that the metastable changes in phonon transmission induced by the irradiation are caused by optically induced changes in the phonon scattering in the GaAs crystal. These changes are such that the TA-phonon transmission along the [100] direction is increased after the irradiation, whereas the $\text{LA}_{[100]}$ -phonon transmission is unchanged within experimental uncertainty.

In Fig. 1(a) the peak time of the TA-phonon signal is seen to change due to the irradiation with 1.06- μm light.

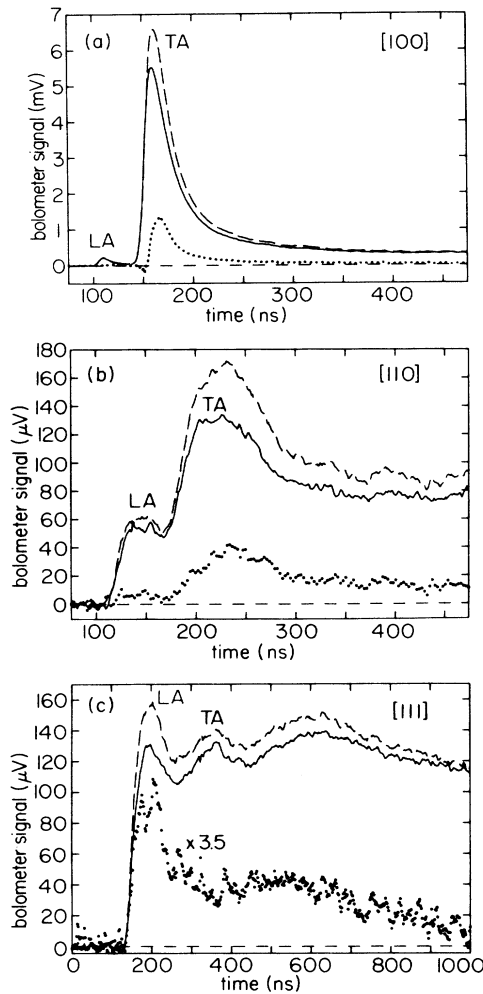


FIG. 1. Acoustic-phonon signal intensity vs transit time across the crystal for the (a) [100], (b) [110], and (c) [111] directions. The solid line is $EL2$ in ground state. The dashed line is $EL2$ in metastable state. The dotted line is the difference between the first two phonon signals; the phonons that are not scattered when $EL2$ is in its metastable state, but are scattered when $EL2$ is in its ground state.

The onset of the change in $TA_{[100]}$ -phonon transmission, as evidenced by the dotted curve (which is the dashed curve minus the solid curve), corresponds to 0.962 ± 0.014 of the velocity of long-wavelength $TA_{[100]}$ phonons. These measurements were performed at a number of laser-pulse energies and consequently varying phonon-energy distributions. The onset of the change in phonon transmission was found to be independent of pulse energy. From the published TA -phonon dispersion curves^{7,8} the onset time for the dotted curve of Fig. 1(a) corresponds to a $TA_{[100]}$ phonon of energy 3.6 ± 1.3 meV. The interpretation of these delayed phonons as higher-energy phonons is consistent with several other observations: The first observation is that increasing the laser-pulse energy results in a broader phonon pulse with more phonons arriving later. This observation is consistent with the existence of more high-energy phonons at higher pulse energies. Conse-

quently the ratio of the amplitude of the high-energy (~ 3.6 meV) phonons [dotted curve in Fig. 1(a)] to the amplitude of the low-energy phonons [solid curve in Fig. 1(a)] should increase with increasing laser-pulse energy. We have verified that this is the case. This second observation rules out diffusive transport which could be used to explain the observed broadening of the phonon signal with increasing pulse energy.

Figures 1(b) and 1(c) show the bolometer response to phonons propagating along the [110] and [111] directions, respectively. Although Figs. 1(b) and 1(c) show well-defined peaks, these peaks are considerably broadened compared to the [100] peaks of Fig. 1(a). This is due to the geometry of our crystal-bolometer system combined with the sharp focusing of [100] phonons relative to the comparatively weakly or even defocused [110] and [111] phonons.

In Figs. 1(b) and 1(c), as in Fig. 1(a), the solid curves were obtained before, and the dashed curves were obtained after the crystal was irradiated with $1.06\text{-}\mu\text{m}$ light for 5 min. The dotted curves are the change in phonon transmission (the solid curves subtracted from the dashed curves). In response to the irradiation an increase in phonon transmission is observed for the $LA_{[110]}$ and fast $TA_{[110]}$ phonons (the weaker slow $TA_{[110]}$ phonon is not resolved). The change in [111] phonon transmission shows no peak when $TA_{[111]}$ phonons are expected to arrive; within experimental uncertainty there is *no measurable change in $TA_{[111]}$ phonon scattering*. A substantial increase in the transmission of $LA_{[111]}$ phonons is seen. It is significant that the irradiation results in no change in the arrival time of these $LA_{[111]}$ phonons. This is in contrast to the $TA_{[100]}$ observations where the delayed TA phonon arrival depended on the dispersion of $\sim 3.6\text{-meV}$ phonons. The dispersion and the corresponding delayed arrival of 3.6-meV $LA_{[111]}$ phonons is negligible. The broad peak arriving after the ballistic LA and TA peaks is interpreted as being due to a combination of multiply internally reflected phonons (involving mode conversion at surfaces), diffusion, and to a lesser extent, possibly phonon dispersion.

From the observed anisotropy of the change in phonon transmission it is possible to determine the symmetry of the responsible defect(s). That we are dealing with a single-defect symmetry seems probable due to the highly anisotropic nature of the change in phonon scattering (no change in $TA_{[111]}$ transmission). The \times 's in Table I mark the TA phonons for the various high-symmetry directions that group theory indicates can couple and thus scatter with three different lattice distortions.^{1,3} The results of our experimental observations are also tabulated. It is clear that the reduction of TA -phonon scattering caused by the irradiation with $1.06\text{-}\mu\text{m}$ light is consistent with a decrease in concentration or scattering cross section of a defect of trigonal symmetry. Defects of tetragonal and orthorhombic symmetry are ruled out. For a trigonal defect it is expected that $LA_{[111]}$ and $LA_{[110]}$ phonons will be scattered, and that $LA_{[100]}$ phonons will not be scattered. Our LA phonon observations are in excellent agreement with these predictions.

The results reported here are closely related to the pres-

TABLE I. Phonon-defect interaction table. The existence of an interaction of a defect of given symmetry with a transverse-acoustic phonon is indicated by an \times . The phonon modes listed are either transverse (T) or fast transverse (FT) polarizations.

Phonon mode	Propagation direction	Tetragonal $\langle 100 \rangle$	Trigonal $\langle 111 \rangle$	Orthorhombic $\langle 110 \rangle$	Experiment
T	[100]		\times	\times	\times
FT	[110]		\times	\times	\times
T	[110]	\times		\times	

ence of the *EL2* defect(s) in our crystal of GaAs. However, when *EL2* is converted to its metastable state, the Fermi level shifts downward,⁹ which may change the phonon scattering cross sections of electrically active defects lying below *EL2* in the energy-band gap. To exhibit anisotropic phonon scattering a defect must have a lower symmetry than the site it occupies.³ This implies the existence of an extended defect and/or a lattice relaxation that lowers the local symmetry. These facts lead us to conclude that shallow effective-mass-like impurities are not responsible for our phonon scattering effects. The defect responsible for the change in scattering must be either *EL2* or another electrically active deep level lying below *EL2* in the energy-band gap. We argue that the scattering of phonons by the *EL2* defect is sufficient to explain the magnitude of the changes in phonon scattering. Light absorption measurements indicate our sample has an *EL2* concentration of $(1-2) \times 10^{16} \text{ cm}^{-3}$. If the phonon scattering cross section of *EL2* in GaAs is of comparable magnitude to those of other deep levels, such as Cr in GaAs,¹ or Sn or Te in $\text{Al}_{0.5}\text{Ga}_{0.5}\text{As}$,¹⁰ then the concentration of *EL2* in our crystal is sufficient to explain the magnitude of the change in phonon scattering we observe. Although no theoretical predictions of the *EL2*-phonon scattering cross section are available, a sizable cross section is suggested by the significant lattice distortions featured in several recently proposed models for this double donor.

The majority of these models propose that *EL2* is an As_{Ga} complexed with other intrinsic defects such as vacan-

cies¹¹⁻¹³ and/or interstitials.¹⁴⁻¹⁶ Of particular interest is a recent electron-nuclear double-resonance (ENDOR) experiment¹⁶ which has been interpreted to show that *EL2* is an As_{Ga} with a neighboring As interstitial positioned to give the overall defect a trigonal symmetry. Similar conclusions have been reached on the basis of annealing studies.^{14,15} We find a definite trigonal symmetry in agreement with the ENDOR results. If there is a family of *EL2* defects^{14,15,17} responsible for the phonon scattering we observe, then the members of this family that dominate the phonon scattering must have the same trigonal defect symmetry.

In conclusion, we have observed phonon scattering effects in LEC-grown semi-insulating GaAs that mirror the metastable, optical-excitation, and thermal-annealing features of the *EL2* defect. The anisotropic increase in phonon transmission caused by the irradiation with 1.06- μm light has been interpreted in terms of the decrease in scattering cross section of, or the removal of, a defect which has trigonal symmetry. This change in phonon transmission does not occur for $\text{TA}_{[100]}$ phonons with energies below $\sim 3.6 \pm 1.3 \text{ meV}$. This energy most probably corresponds to an electronic energy-level splitting of the defect's ground state.

We gratefully acknowledge helpful discussions with P. B. Klein, T. A. Kennedy, N. D. Wilsey, and Pay-June Lin-Chung, and S. Kirchoefer for technical assistance.

¹V. Narayanamurti, M. A. Chin, and R. A. Logan, *Appl. Phys. Lett.* **33**, 481 (1978).

²H. Tokumoto and T. Ishiguro, *J. Phys. Soc. Jpn.* **46**, 84 (1979); **46**, 1944(E) (1979).

³A. S. Nowick and W. R. Heller, *Adv. Phys.* **14**, 101 (1965); C. A. Bates, *Phys. Rep.* **35C**, 187 (1978).

⁴K. Weiser, U. Strom, S. A. Wolf, and D. U. Gubser, *J. Appl. Phys.* **52**, 4888 (1981).

⁵J. C. Culbertson, U. Strom, P. B. Klein, and S. A. Wolf, *Phys. Rev. B* **29**, 7054 (1984).

⁶G. Vincent, D. Bois, and A. Chantre, *J. Appl. Phys.* **53**, 3643 (1982).

⁷J. L. T. Waugh and G. Dolling, *Phys. Rev.* **132**, 2410 (1963).

⁸E. N. Korol, *Fiz. Tverd. Tela* **12**, 644 (1970) [*Sov. Phys. Solid State* **12**, 497 (1970)].

⁹Ralph Bray, K. Wan, and J. C. Parker, *Phys. Rev. Lett.* **57**, 2434 (1986).

¹⁰V. Narayanamurti, R. A. Logan, and M. A. Chin, *Phys. Rev. Lett.* **43**, 1536 (1979).

¹¹J. Lagowski, M. Kaminska, J. Parsey, H. C. Gatos, and

W. Walukiewicz, in *Gallium Arsenide and Related Compounds*, edited by G. E. Stillman, IOP Conf. Proc. No. 65 (Institute of Physics, Bristol, 1983).

¹²Y. Zou, J. Shou, Y. Lu, K. Wang, B. Yu, B. Lu, C. Li, L. Li, J. Shao, and C. Sheng, *J. Electron. Mater.* **14a**, 1021 (1985).

¹³J. A. van Vechten, in *Microscopic Identification of Electronic Defects in Semiconductors*, edited by N. M. Johnson, S. G. Bishop, and G. D. Watkins (Materials Research Society, Warrendale, 1985), Vol. 46, p. 83.

¹⁴T. Ikoma, M. Taniguchi, and Y. Mochizuki, *Gallium Arsenide and Related Compounds 1984*, IOP Conf. Ser. No. 74 (IOP, Bristol, 1984), Chap. 2.

¹⁵H. J. von Bardeleben, D. Stievenard, D. Deresmes, A. Huber, and J. C. Bourgoin, *Phys. Rev. B* **34**, 7192 (1986).

¹⁶B. K. Meyer, D. M. Hofmann, and J.-M. Spaeth, in *Defects in Semiconductors*, edited by H. J. von Bardeleben (Trans. Tech. Publications Ltd., Aedermannsdorf, Switzerland, 1986), p. 311.

¹⁷D. Vignaud and J. L. Farvacque, *Solid State Commun.* **60**, 527 (1986).